Comparison of the Allosteric Properties of the Co(II)- and Zn(II)-Substituted Insulin Hexamers†

Curtis R. Bloom,‡,§ Nancy Wu,‡ Alex Dunn,‡,§ Niels C. Kaarsholm,*,|| and Michael F. Dunn*,‡

Department of Biochemistry, University of California, Riverside, California 92521, and Novo Research Institute, Novo Nordisk A/S, DK-2880 Bagsvaerd, Denmark

Received January 9, 1998; Revised Manuscript Received May 12, 1998

ABSTRACT: The positive and negative cooperativity and apparent half-site reactivity of the Co(II)-substituted insulin hexamer are well-described by a three-state allosteric model involving ligand-mediated interconversions between the three states: $T_3T_3' \rightleftharpoons T_3°R_3° \rightleftharpoons R_3R_3'$ [Bloom, C. R., Heymann, R., Kaarsholm, N. C., and Dunn, M. F. (1997) *Biochemistry 36*, 12746−12758]. Because of the low affinity of the T state for ligands, this model is defined by four parameters: L_o^A and L_o^B, the allosteric constants for the T_3T_3' to $T_3°R_3°$ and the $T_3°R_3°$ to R_3R_3' transitions, respectively, and the two dissociation constants for ligand binding to $T_3°R_3°$ and to R_3R_3'. The d−d electronic transitions of the Co(II)-substituted hexamer give optical signatures of the T to R transition which can be quantified, but the "spectroscopically silent" character of Zn(II) has made previous attempts to describe the Zn(II) species difficult. This work shows that the T to R state conformational transitions of the Zn(II) hexamer can be easily quantified using the chromophore 4-hydroxy-3-nitrobenzoate (4H3N). When the chromophore is bound to the HisB10 sites of the R state, the absorption spectrum of 4H3N is red-shifted, exhibiting strong absorbance and CD signals, whereas 4H3N does not bind to the T state. Hence, 4H3N can be employed as a sensitive indicator of conformation under conditions that do not significantly disturb the T to R state equilibrium. Using 4H3N as an indicator, these studies show that both L_o^A and L_o^B are made less favorable by the substitution of Co(II) for Zn(II); L_o^A is increased by 10-fold while L_o^B by 35-fold, whereas the ligand affinities of the phenolic pockets are unchanged.

The insulin hexamer has become one of the most sophisticated allosteric systems for which quantitative modeling has been carried out (*2*−*5*). The presence of positive and negative homotropic and heterotropic interactions within a single oligomeric ligand binding protein provides the opportunity to test hypotheses concerning the origins of negative homotropic interactions. Insulin allostery has been shown to be important to the physicochemical stability of insulin formulations used in the treatment of diabetes (*6*), and likely is important for the storage of insulin in secretory vesicles in vivo. Most of the previous studies of the allosteric mechanism for the insulin hexamer utilized the optical properties of Co(II)-substituted hexamers to make possible quantitative data collection (*2*−*4*, *7*, *8*). The use of Co(II) has allowed investigation of the effects of polypeptide mutations, changes in ligand structure, and homotropic and heterotropic ligand interactions. The effects of mutation and ligand structure have been quantified for the Co(II)-substituted hexamer using the suboptimal symmetry model of Seydoux, Malhotra, and Bernhard (the SMB model) (*2*−*4*, *9*).

The insulin hexamer exists in three distinct global conformations designated T_3T_3',[1] $T_3°R_3°$, and R_3R_3' (*1*−*7*). These conformations have been identified and extensively characterized, both in the crystalline state (*10*−*16*) and in solution (*1*, *2*, *6*−*8*, *17*−*19*).

Insulin hexamers are assembled as interdigitated asymmetric trimers arranged about an exact 3-fold symmetry axis[2] (Figure 1) (*10*−*14*, *20*, *21*). In the T to R state allosteric transition, residues B1−B9 become helical, hydrophobic pockets capable of binding phenol and phenolic derivatives are formed at the subunit interfaces (the phenolic pockets), and the HisB10 divalent metal ion sites are converted from an octahedral $M^{2+}(N_3O_3)$ ligand field residing in shallow depressions at either end of the hexamer to tetrahedral or

† This work was supported by a gift from the Novo Research Institute.

* To whom correspondence should be sent: Department of Biochemistry, University of California, Riverside, CA 92501. Telephone: (909) 787-4235. Fax: (909) 787-3590. E-mail: Dunn@ucrac1.ucr.edu.

‡ University of California.

§ Current address: Department of Chemistry, California Institute of Technology, Pasadena, CA 91125.

|| Novo Nordisk A/S.

[1] The global conformations of insulin hexamers with extended (T) and α-helical (R) conformations of B chain residues 1−8 are designated T_6, T_3R_3, and R_6 (*1*). T_3T_3' and R_3R_3' designate conformations with one 3-fold axis and three pseudo-2-fold axes of symmetry, while $T_3°R_3°$ designates the hexamer with only a single, 3-fold axis of symmetry (*2*). L_o^A and L_o^B are the allosteric constants for the interconversion of T_3T_3' with $T_3°R_3°$ and $T_3°R_3°$ with R_3R_3', respectively. $K_R°$, K_R, and K_R' are the dissociation constants for ligand binding to the phenolic pockets of the $R_3°$, R_3, and R_3' units of $T_3°R_3°$ and R_3R_3', respectively. K_T is the dissociation constant for the binding of phenolic ligands to trimeric units in the T state conformation. ρ is the fraction of R state species. PABA is *p*-aminobenzoic acid. 4H3N is 4-hydroxy-3-nitrobenzoate. 2,6- and 2,7-DHN are 2,6- and 2,7-dihydroxynaphthalene, respectively.

[2] This symmetry is strictly adhered to in rhombehedral crystals, whereas there are slight deviations from true 3-fold symmetry in monoclinic crystals of the insulin hexamer.

S0006-2960(98)00071-3 CCC: $15.00
Published on Web 07/10/1998

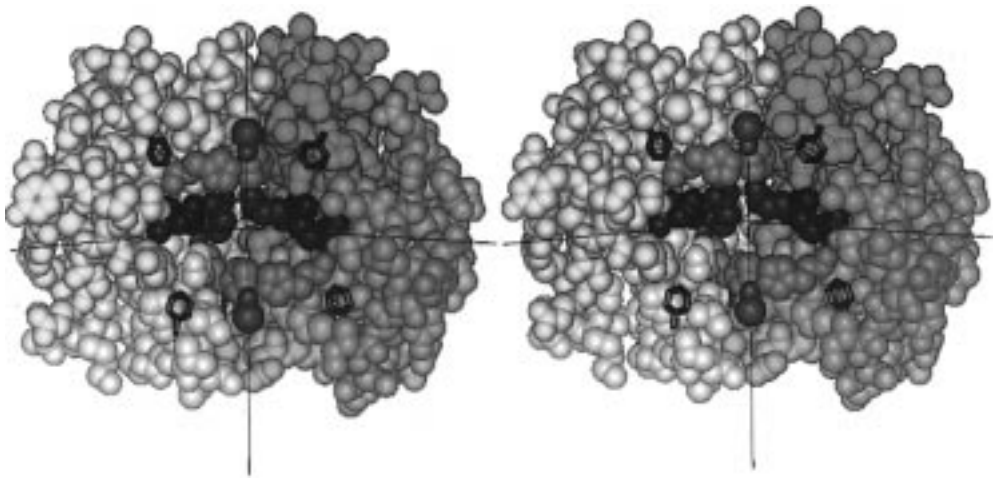

FIGURE 1: Space fillling stereodiagram of the R_6 insulin hexamer (R_3R_3') viewed along one of the three pseudo-2-fold axes oriented perpendicular to the hexamer 3-fold axis. Individual subunits are shown in red, light blue, gray, and yellow. In this view, one dimeric unit is cut away, exposing four of the six essentially identical phenolic pockets and the HisB10 sites. The phenolic pockets are shown occupied by molecules of phenol (shown as black ball-and-stick structures). As is evident in this diagram, each phenolic pocket is located on a dimer−dimer interface. The HisB10 zinc ions (purple balls) are located about 16 Å apart on the 3-fold symmetry axis, and each zinc ion is shown coordinated to a chloride ion (dark blue balls). The HisB10 side chains are shown in green and the GluB13 side chains in black. Each chloride ion is positioned at the bottom of a 8−12 Å tunnel extending along the 3-fold axis from the surface to the metal ion. Coordinates were provided courtesy of G. David Smith.

five-coordinate $M^{2+}(N_3X)$ or $M^{2+}(N_3XY)$ ligand fields located at the bottom of narrow, 12 Å deep pockets oriented along the 3-fold symmetry axis (where N is His nitrogen, O is H_2O, and X and Y are exogenous ligands). The R state phenolic pockets comprise one class of allosteric ligand binding sites. The second class of allosteric sites involves the binding of anions to the R state HisB10 sites. These two classes of sites show strong heterotropic interactions.

Bloom et al. (*2*−*4*) and Brzović et al. (*7*) have shown that the allosteric properties of the insulin hexamer consisting of half-site reactivity and mixed positive and negative cooperativity can be described well by the SMB model (Figure 2). The treatment of Bloom et al. (*2*−*4*) proposes preexisting equilibria among the three allosteric states of the insulin hexamer, i.e., $T_3T_3' \rightleftharpoons T_3°R_3° \rightleftharpoons R_3R_3'$. Under the assumption that allosteric ligands bind only to the ligation sites of $R_3°$, R_3, and R_3' units, then the homotropic allosteric effects of phenolic ligands could be modeled by invoking four parameters: two allosteric constants, $L_o^A = [T_3°R_3°]/[T_3T_3']$ and $L_o^B = [R_3R_3']/[T_3°R_3°]$, and two dissociation constants, $K_R°$, the dissociation constant for ligand binding to $T_3°R_3°$, and K_R, the dissociation constant for ligand binding to R_3R_3'.

One of the most interesting properties of the insulin hexamer is the ability of the HisB10 sites to undergo a conformation-mediated switch between octahedral and tetrahedral coordination geometries. Ligation both to the phenolic sites and to the HisB10 sites modulates the equilibrium between octahedral and tetrahedral complexes. Co(II) substitution provides a chromophoric probe of the insulin conformational state that is based on the unique spectroscopic signatures of the octahedral and tetrahedral (or five-coordinate) ligand fields (*2*−*4*, *7*, *18*−*25*). Thus, most studies of the allosteric properties of the insulin hexamer have relied on the spectroscopic signatures of the Co(II) hexamer to generate signals of conformation (*2*−*4*, *18*, *19*, *23*, *24*). However, Rauhel-Clermont et al. (*6*) have shown that substitution of Co(II) for Zn(II) alters the relative stabilities of the three insulin hexamer conformations.[3] Furthermore, since Zn(II) is the in vivo metal ion for the insulin hexamer, it is important to quantify the allosteric properties of the Zn(II)-substituted species. Although Co(II) and Zn(II) exhibit very similar ionic radii (0.72 and 0.74 Å, respectively), the relative affinities for ligands are different, and therefore, observable differences are seen in the strengths with which ligands bind to the fourth coordination position of the R state sites (*8*).

Huang et al. (*8*) have introduced the chromophoric ligand, 4-hydroxy-3-nitrobenzoate (4H3N), as a new probe of ligand binding to the HisB10 sites of R state insulin hexamers. To quantify differences between the Co(II) and Zn(II) hexamers, we have extended the use of 4H3N as a chromophoric signal of the T to R state conformational change at the R state HisB10 sites. Herein, the spectroscopic properties of 4H3N are exploited to measure the concentration of the R state present in solution, yielding data which then can be analyzed both to characterize ligand binding interactions for the Zn(II) hexamer and to quantify the differences between the Co(II) and Zn(II) insulin hexamers. It will be shown that the substitution of Co(II) for Zn(II) makes the allosteric transitions to the R state less favorable and, therefore, that the HisB10 metal ion also is an effector of insulin allostery.

[3] Co(II) and Zn(II) differ in their electronic configurations. Co(II) with an $[Ar]3d^7$ configuration has two unfilled 3d orbitals, while Zn(II) with a $[Ar]3d^{10}$ configuration has a completely filled 3d shell. Thus, ligation of Co(II) to electron-donating species is complicated by the symmetry of the ligand field, spin−orbit coupling, and Jahn−Teller effects, while ligation to Zn(II) involves the vacant 4s orbital and, therefore, is unperturbed by d orbital considerations and ligand field effects. Due to the directional nature of d orbitals, ligation to Co(II) is predicted to favor orientations that align the unfilled orbitals with incoming ligands. The spherical nature of the Zn(II) 4s orbital renders ligation independent of orientation, as long as the +2 charge on the metal center is dissipated and unfavorable ligand interactions are minimized.

EXPERIMENTAL PROCEDURES

Materials

Metal-free GluA17Gln mutant insulin and wild-type human insulin were supplied by the Novo Research Institute (Bagsvaerd, Denmark). $Co(ClO_4)_2$ (Alfa, Danvers, MA), $ZnSO_4$ (Mallinckrodt, St. Louis, MO), KSCN (Aldrich, Milwaukee, WI), PABA (Aldrich), resorcinol (Sigma), Trizma (Sigma), $HClO_4$ (Mallinckrodt), 2,7-dihydroxynaphthalene (Sigma), 2,6-dihydroxynaphthalene (Aldrich), and phenol (Aldrich) were used without additional purification.

Methods

UV−Vis Absorption Studies of the Insulin 3-Nitro-4-hydroxybenzate (4H3N) System. Absorbance spectra for a 0.1 mM solution of 4H3N alone and in the presence of 1.0 mM Zn(II) wild-type insulin hexamers with 100 mM phenol using 50 mM Tris-perchlorate buffer (pH 8.0) were measured on a HP8452A diode array spectrophotometer equipped with a computerized data processing system. Difference spectra are calculated by subtracting the absorbance of free 4H3N from the absorbance of bound 4H3N ($A_{free} - A_{bound} = \Delta A_{abs.}$).

Comparison of the Co(II) Data for the UV−Vis Absorption and CD Signatures for the T to R Allosteric Transitions to the Data for the 4H3N Signature. Isotherms for the binding of phenol to Co(II) wild-type insulin hexamers in the presence of 5 mM *p*-aminobenzoate (PABA) were determined as previously described (*2*, *3*, *18*) except for the presence of 0.15 mM 4H3N. Absorption titration progress generally was monitored both at A_{572} [for the Co(II) d−d transitions] and at A_{444} (for the 4H3N chromophoric shift). Circular dicroism spectra were measured over the range of 340−550 nm for the Zn(II) hexamer and over the range of 340−700 nm for the Co(II) hexamer using a JASCO J-715 spectropolarimeter calibrated with (+)-10-camphorsulfonic acid. The CD is expressed as $\Delta\epsilon$ in units of M^{-1} cm^{-1}; i.e., $\Delta\epsilon = \theta/(32980Lc)$, where θ is the ellipticity, L is the cell path length, and c is the molar concentration of chromophore, in this case, 4H3N.

UV−Vis Absorption and CD Binding Isotherms. UV−vis absorbance isotherms for the phenol-, resorcinol-, and 2,7-DHN-driven T to R state transitions of Co(II)-substituted wild-type insulin and GluA17Gln mutant insulin generally were determined as described by Choi et al. (*18*) and Bloom et al. (*2*, *3*). Isotherms for the Zn(II)-substituted wild-type and GluA17Gln mutant insulins were determined by monitoring the 4H3N signal at 444 nm due to 4H3N at increasing concentrations of the phenolic ligand. Concentrations of wild-type insulin and GluA17Gln mutant insulin were determined by absorbance measurements ($\epsilon_{280} = 5800$ M^{-1} cm^{-1}) (*26*).

The CD isotherms were determined at wavelengths selected to give signatures of either 4H3N or Co(II) d−d transitions. All of the isotherms were measured in 50 mM Tris-ClO_4 buffer at pH 8.0 using 0.33 mM Co(II) hexamer concentrations in the presence of 2 mM $PABA^-$.

RESULTS

Spectral Characterization of 4-Hydroxy-3-nitrobenzoate. The UV−vis absorbance spectrum for 4H3N in 50 mM Tris-ClO_4 (pH 8.0) possesses a characteristic band centered at

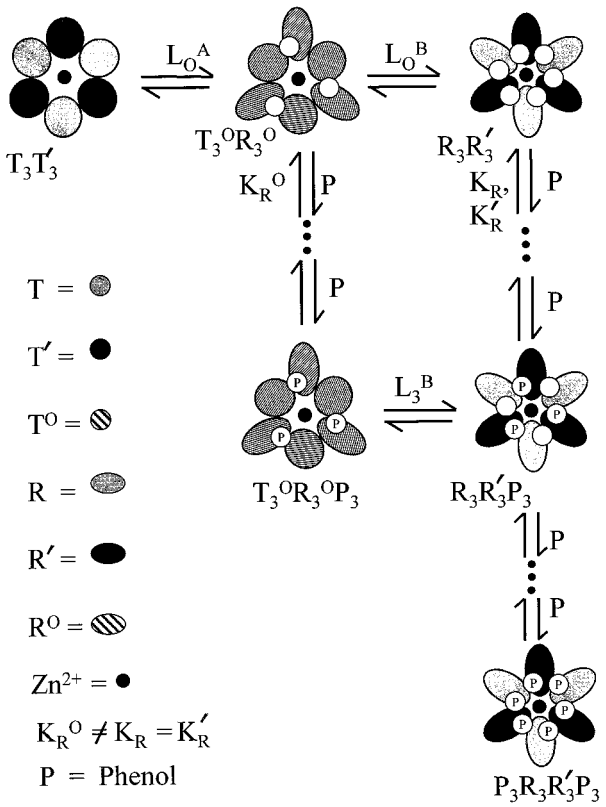

FIGURE 2: Cartoon depicting the symmetry properties of the insulin hexamer allosteric states, the binding sites for phenolic ligands (P), and the complex equilibria for interconversion of T_6, T_3R_3, and R_6, coupled to ligand binding steps for each R state conformation. The interconversions of the T_3T_3', $T_3°R_3°$, and R_3R_3' states are shown as concerted processes. Ligand binding to each class of sites consists of independent and identical processes (see the text).

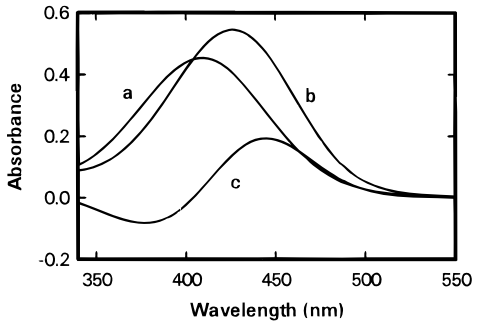

FIGURE 3: UV−visible absorbance spectra of 4H3N (a) free and (b) in the presence of the wild-type Co(II) insulin hexamer with 100 mM phenol and 50 mM Tris-ClO_4^- buffer at pH 8.0. The calculated difference spectra (c) ($A_{free} - A_{bound}$) exhibits a maximum ΔA at 444 nm.

410 nm ($\epsilon_{410} = 4.3 \times 10^3$ M^{-1} cm^{-1}) (Figure 3a). Upon excess Co(II) wild-type insulin hexamer being mixed with 50 mM phenol, conditions which give Co(II)−R_6 (*7*, *17*, *23*−*25*), the absorbance peak shifts from 410 to 426 nm ($\epsilon_{426} = 5.2 \times 10^3$ M^{-1} cm^{-1}) (Figure 3b). The calculated difference spectrum (c) has a λ_{max} of 444 nm. Previous characterization of the 4H3N−Co(II) R state insulin complex shows a Co(II) d−d spectral envelope ($\lambda_{max} = 536$ nm, $\epsilon_{536} = 273$ M^{-1} cm^{-1}, $\lambda_{max} = 572$ nm, and $\epsilon_{572} = 243$ M^{-1} cm^{-1}) (*8*), a finding consistent with the assignment of a pentahedral ligand field to the complex, with 4H3N coordination via a bidentate carboxylate. The Zn(II)-substituted insulin hexamer also was found to give a complex with 4H3N exhibiting UV−vis

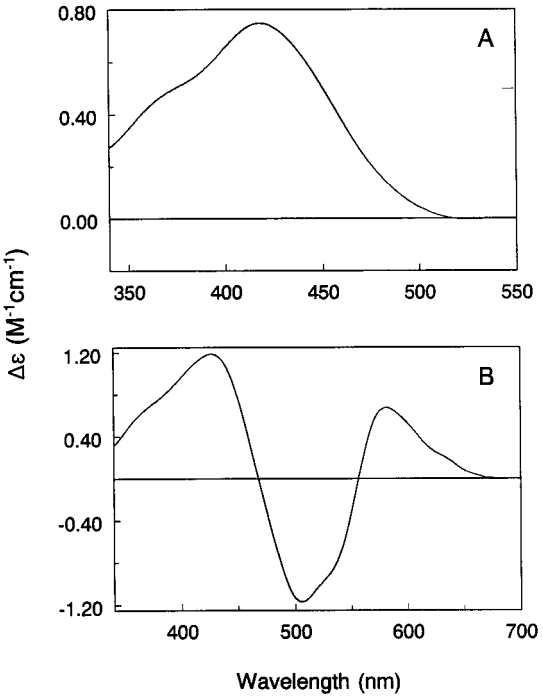

FIGURE 4: CD spectra of 4H3N bound to the HisB10 sites of (A) the Zn(II)−R_6 and (B) the Co(II)−R_6 hexamers employing 2 mM insulin and 0.65 mM Zn^{2+} (A) or Co^{2+} (B), 2 mM PABA, 0.15 mM 4H3N, and 10.6 (A) or 24.9 mM (B) phenol, in 50 mM Tris-ClO_4^- at pH 8.0.

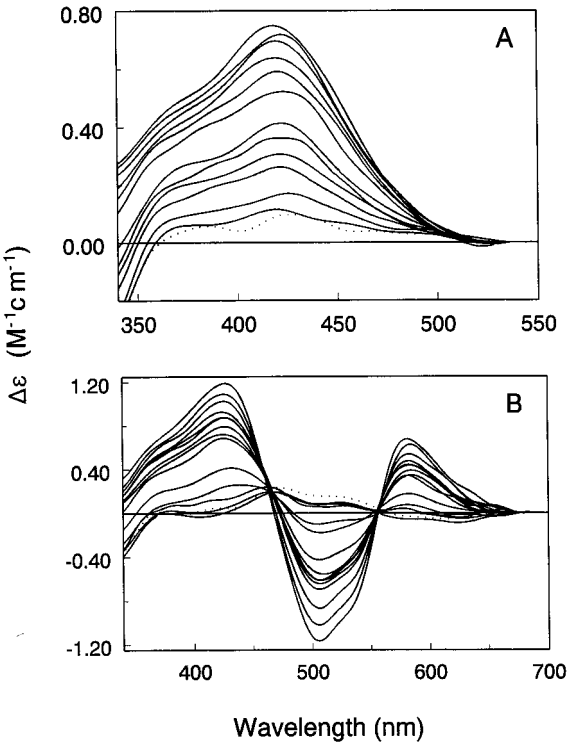

FIGURE 5: CD spectra measured as a function of [phenol] for the Zn(II) insulin hexamer (A) and for the Co(II) insulin hexamer (B). Samples contain 2 mM insulin, 0.65 mM Zn^{2+} (A) or Co^{2+} (B), 2 mM PABA, and 0.15 mM 4H3N in 50 mM Tris-ClO_4^- at pH 8.0. The dotted curves show the spectra prior to the addition of phenol. In panel A, the family of curves represents additions of phenol in the 0.1−10.6 mM range, while in panel B, additions between 0.2 and 24.9 mM are employed.

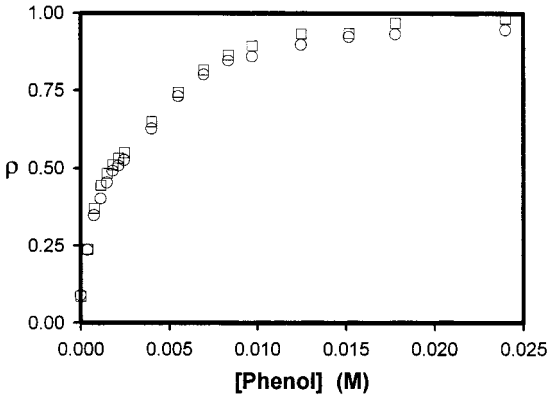

FIGURE 6: Phenol titration of Co(II) wild-type insulin with 5 mM PABA monitored by signals derived from the d−d Co(II)−PABA transitions and from the spectral change of 4H3N. The titration is plotted as the fraction of R state (ρ) vs [phenol] for a solution containing 0.33 mM Co(II) insulin hexamer, 5 mM PABA, and 0.15 mM 4H3N in 50 mM Tris-ClO_4^- at pH 8.0. The fraction of total R state (ρ) is defined as the relative absorbance change at 444 nm (○) due to the chromophoric shift of the 4H3N spectra or the relative absorbance change at 572 nm (□) from the R state Co(II)−PABA d−d transition spectra. For the Co(II) insulin titrations, the fraction of R state is determined as described by Choi et al. (*18*).

absorption spectral properties essentially identical to those shown in Figure 3 for the Co(II) system (data not shown).

The spectral shift of 4H3N is dependent on the phenolic ligand-induced allosteric transitions of the insulin from the T state to the R state. Control experiments (data not shown) established that, under the experimental conditions of these studies, there is no evidence of interactions directly between phenol, resorcinol, or the DHNs and 4H3N that give rise to a red-shifted 4H3N absorption spectrum or a CD spectrum.

Figure 4A shows the CD spectrum of 4H3N complexed to the Zn(II)-substituted insulin hexamer in the presence of 2 mM PABA and 10.6 mM phenol. The spectrum is characterized by a peak with a λ_{max} of 420 nm due to the induced structural asymmetry of the 4H3N chromphore bound to the HisB10 sites of the R state hexamer. The shoulder to this peak located at ∼370 nm likely indicates splitting of the $\pi-\pi^*$ transition for the bound chromophore. Figure 4B shows the CD spectrum of the corresponding Co(II)-substituted complex of 4H3N. This spectrum is similarly characterized by prominent features located at ∼370 (shoulder) and 420 nm (positive peak), together with peaks at 500 (negative) and 590 nm (positive). By comparison to the Zn(II) system, the 420 nm peak and the 370 nm shoulder are assigned to an induced asymmetry of the 4H3N complex at the HisB10 site, while the features at 500 and 590 nm are due to the Co(II) d−d transitions. When the CD spectra are measured as a function of the concentration of phenol, the Zn(II) system (Figure 5A) shows that the peak due to 4H3N at 420 nm increases and then becomes essentially independent of phenol as the concentration of phenol is increased. The Co(II) system gives a more complex set of spectral changes (Figure 5B), showing apparent isosbestic points located at ∼465 and ∼565 nm reflecting the interconversion of the CD spectrum of Co(II)−T_6 with the spectrum of the product Co(II)−R_6−4H3N complex. Again, the amplitudes of the changes in the spectrum approach saturation at high concentrations of phenol.

Comparison of the 4H3N and Co(II) Spectral Signatures. The correlation of the R state conformation with the tetrahedral or pentacoordinate Co(II) UV−vis absorption

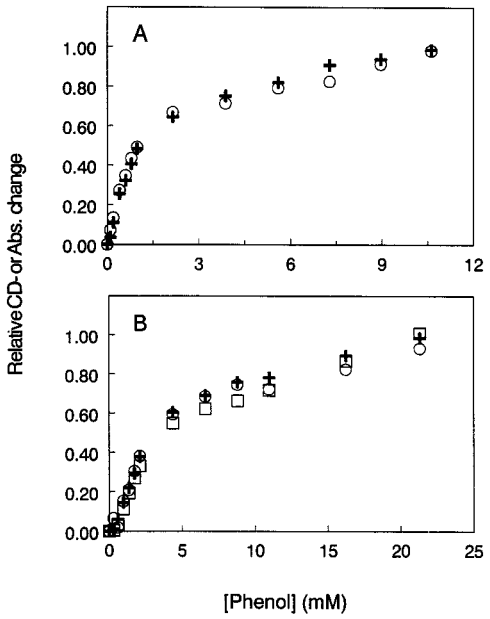

FIGURE 7: Isotherms comparing absorbance and CD changes (normalized) as a function of [phenol] for the Zn(II) (A) and Co(II) (B) hexamers. Concentrations of insulin, metal ion, PABA, and 4H3N are as shown in Figure 5. Panel A compares the absorbance change at 440 nm (○) with the CD change at 420 nm (+) for the 4H3N chromophore. For the Co(II) system, panel B compares 4H3N changes in absorbance at 440 nm (○) and CD at 420 nm (+) with the CD changes at 500 nm (□) derived from the Co^{2+} chromophore.

spectrum signature is well established (*2*−*4*, *17*−*19*, *25*). Figure 6 establishes that the appearances of the R state, as determined from the d−d envelope of the Co(II)−PABA absorbance spectrum (□) (λ_{max} = 572 nm) or from the absorbance change at 444 nm (○) due to the 4H3N complex, give identical isotherms (within experimental error). Similarly, when the absorption and CD signals for the Zn(II) system are compared (Figure 7A), it is evident that the normalized absorption changes and the normalized CD changes give essentially identical isotherms. Furthermore, for the Co(II) system, the relative absorption and relative CD changes for the 4H3N signatures give identical isotherms, which coincide with the d−d transition CD changes (Figure 7B).

Ligand Binding to Co(II)- and Zn(II)-Substituted Wild-Type Insulin and GluA17Gln Mutant Insulin Hexamers. Absorbance isotherms for the binding of resorcinol, phenol, or 2,6-DHN to Co(II)- and Zn(II)-substituted wild-type insulins (Figure 8) and GluA17Gln mutant insulin (Figure 9) are shown. Curve fitting to the equation for the fraction of the R state (ρ), eq 1 (*2*, *4*) (see Figure 2)

$$\rho = \frac{0.5L_o^{B}(1+\beta)^3 + (1+\alpha)^6}{L_o^{B}(1+\beta)^3 + (1+\alpha)^6 + L_o^{B}L_o^{A}} \qquad (1)$$

where α = [phenolic ligand]/K_R and β = [phenolic ligand]/K_R^o, is shown for each isotherm (solid lines), and the results are summarized in Table 1. All isotherms for wild-type Co(II) hexamers give values for L_o^A of (40 ± 20) and for L_o^B of (3 ± 1.5) × 10^7, while the corresponding Zn(II) hexamers give values for L_o^A of (5 ± 2) and for L_o^B of (8 ± 4) × 10^5 (Table 1). The isotherms for the Co(II)-substituted GluA17Gln mutant insulin hexamer all give values for L_o^A of (1 ± 0.5) × 10^2 and for L_o^B of (4 ± 2) × 10^7, while the corresponding Zn(II) GluA17Gln mutant hexamers give values for L_o^A of (9 ± 4.5) and for L_o^B of (1 ± 0.5) × 10^6 (Table 1).

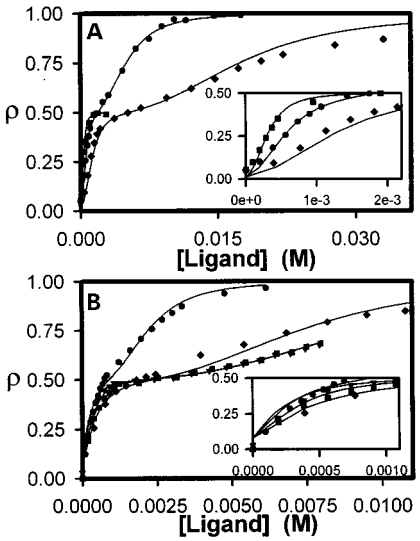

FIGURE 8: Ligand titrations for Co(II) wild-type insulin with 2 mM PABA (A) and Zn(II) wild-type insulin with 2 mM PABA (B) using 0.15 mM 4H3N as an indicator. Titrations are plotted as the fraction of R state (ρ) vs $[ligand]_{free}$ for solutions containing 0.33 mM insulin hexamer in 50 mM Tris-ClO_4^- at pH 8.0. For the Zn(II) insulin titrations, the fraction of total R state (ρ) is defined as the relative absorbance change at 444 nm, due to the chromophoric shift of the 4H3N spectra. For the Co(II) insulin titrations, the fraction of R state is determined as described by Choi et al. (*18*). (A) Binding isotherms for the (●) resorcinol-, (■) 2,6-DHN-, and (◆) phenol-mediated allosteric transitions of Co(II) wild-type insulin (the inset shows the expanded first binding phase). Binding curves (solid lines) were calculated for eq 1 assuming identical allosteric parameters (L_o^A = 1 × 10^2, and L_o^B = 4 × 10^7) using the software Peakfit (Jandel Corp.). (B) Binding isotherms for the (●) resorcinol-, (■) 2,6-DHN-, (▽) 2,7-DHN-, and (◆) phenol-mediated allosteric transitions of Zn(II) wild-type insulin. Binding curves (solid lines) were calculated using identical allosteric parameters characteristic of the Zn(II) wild-type insulin in 2 mM $PABA^-$ (assuming L_o^A = 9 × 10^6 and L_o^B = 1 × 10^6) and show an excellent correlation with the observed data (r^2 > 0.97).

DISCUSSION

4H3N Is a Chromophoric Indicator of the T to R State Allosteric Transition of the Insulin Hexamer. To qualify as a useful chromophoric indicator of the multiple equilibria involved in the T to R state allosteric transition of the insulin hexamer, 4H3N must meet the following criteria. (a) Binding of 4H3N must distinguish between the T and R states with high specificity. The studies of Huang et al. (*8*) establish that this criterion is met. 4H3N binds to the HisB10 sites of R state hexamers but not to the T state hexamers. (b) Binding must cause a significant perturbation of a diagnostic spectroscopic signal such as the 4H3N UV−vis absorption or CD spectrum. Both the relatively intense π−π* transition of 4H3N and the red shift of this band when complexed to the HisB10 site and the induced CD of the complex (Figures 4, 5, and 7) fulfill this criterion. (c) To qualify as a useful spectroscopic probe, the amplitude of the spectroscopic signal resulting from binding must provide a sufficiently sensitive signal to allow 4H3N to be used as an indicator of the distribution of hexamer conformations while

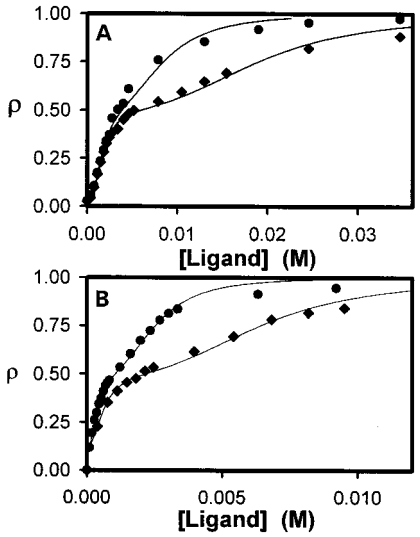

FIGURE 9: Ligand titrations for Co(II) GluA17Gln mutant insulin with 2 mM PABA (A) and Zn(II) GluA17Gln mutant insulin with 2 mM PABA (B) using 0.15 mM 4H3N as an indicator. Titrations are plotted as the fraction of R state (ρ) vs $[ligand]_{free}$ for solutions containing 0.33 mM insulin hexamer in 50 mM Tris-ClO_4^- at pH 8.0. (A) Binding isotherms for the (●) resorcinol- and (◆) phenol-mediated allosteric transitions of Co(II) GluA17Gln mutant insulin (the inset shows the first binding phase on an expanded scale). Binding curves (solid lines) were calculated for eq 1 assuming identical allosteric parameters ($L_o^A = 40 \times 10^7$, and $L_o^B = 3 \times 10^7$) using the software Peakfit (Jandel Corp.). (B) Binding isotherms for the (●) resorcinol- and (◆) phenol-mediated allosteric transitions of Zn(II) GluA17Gln mutant insulin. Binding curves (solid lines) were calculated using identical allosteric parameters characteristic of the Zn(II) wild-type insulin in 2 mM $PABA^-$ (assuming $L_o^A = 5 \times 10^5$ and $L_o^B = 8 \times 10^5$) and show an excellent correlation with the observed data ($r^2 > 0.99$).

introducing only a negligible perturbation of that distribution. As discussed below, this criterion is met both for the change in UV−vis absorption and for the change in CD.

The absorbance spectrum for the 4H3N dianion free in solution at pH 8.0 is characterized by a maximum at 410 nm ($\epsilon_{410} = 4.3 \times 10^3\ M^{-1}\ cm^{-1}$) that is well separated both from the hexamer spectrum and from the Co(II) d−d transitions (Figure 3a). Upon mixing with R state Co(II) insulin hexamers, the λ_{max} of 4H3N shifts to 426 nm (Figure 3b), and absorbance bands characteristic of a pentahedral Co(II) complex ($\lambda_{max} = 532$ and 572 nm) are observed (*8*). In contrast, no evidence of binding to the T state was found. Therefore, the $A_{free} - A_{bound}$ difference spectrum resulting from the binding of 4H3N possesses a maximum at 444 nm (Figure 3c) and is diagnostic of the R state hexamer. It previously has been established that 4H3N binds to R_6 with a stoichiometry of two molecules of 4H3N per hexamer (one per HisB10 site) (*8*).

Comparison of the titrations of the Co(II)-substituted wild-type insulin hexamer carried out under conditions where the isotherm could be followed either by the changes in the Co(II) d−d transitions at 572 nm (the maximum of the PABA complex) or by the changes in the spectrum of 4H3N (difference spectrum maximum at 444 nm) (Figure 6) establishes that the ΔA_{444} signal from 4H3N gives, within experimental error, an isotherm identical to that obtained from the Co(II) signal.[4] Furthermore, inspection of the Co(II) d−d transitions measured in the absence and presence of 4H3N shows the isotherms to be identical, indicating that under the experimental conditions used in Figure 6 perturbations due to the binding of 4H3N are negligible. Therefore, it is clear that the 4H3N signal meets the criteria necessary to qualify as an indicator which may be used to quantify the T to R state allosteric transitions of the Co(II)- and Zn(II)-substituted insulin hexamers.

4H3N Is a Sensitive Circular Dichroism Probe of the T to R State Allosteric Transition. To be an effective CD probe, the induced CD must give a transition of sufficient intensity to allow detection when only a small fraction of the sites are occupied by 4H3N.

The CD spectra presented in Figures 4 and 5 demonstrate that 4H3N binding to the HisB10 sites provides sensitive signatures of the R state conformation. The CD spectral features assigned to the $\pi-\pi^*$ transition of the bound 4H3N dianion have their origins in the structural asymmetry induced by the chirality of the HisB10 site. The isotherms presented in Figures 6 and 7 establish a direct one-to-one correlation between the UV−vis absorption changes in the spectrum of 4H3N and the CD changes for both the Co(II)- and Zn(II)-substituted systems and between the CD and absorbance spectra of the 4H3N chromphore and the CD spectra of the Co(II) d−d transitions (Figure 7). These correlations provide additional evidence indicating that the spectroscopic signatures which accompany the conversion of the metal center at the HisB10 site from an octahedral geometry to tetrahedral or pentacoordinate provide valid spectroscopic signatures which can be used to quantify the extent of the T to R state conformational transition.

Comparisons of Wild-Type and the GluA17Gln Mutant Insulins. In T_6 crystal structures determined between pH 6.0 and 7.0 by X-ray difraction, GluA17 makes a salt bridge interaction with the α-NH_3^+ of PheB1 together with the side chain of ArgB22 (*10*). (The T_6 structure of pig insulin shows that the side chain of ArgB22 takes up two conformations, one involving charge−charge interactions with the side chain of GluA17 and one where the ArgB22 side chain is rotated away.) The 20−30 Å displacement of PheB1 resulting from the coil to helix transition accompanying the T to R state interconversion destroys these salt bridging interactions. Since the replacement of Glu by Gln at position A17 eliminates the A17−B1−B22 salt bridges, this mutation might be expected to destabilize the T state. The side chain of A17 lies on the surface of the hexamer at a location that is distant from both the phenolic pockets and the HisB10 sites; hence, mutations at this position are not predicted to alter the structures of either the phenolic pocket or the HisB10 site. Consequently, the K_R and K_R^o values for the binding of phenolic ligands should be unaffected by the A17 mutation.

[4] The crystal structure of the Zn(II)−$T_3^oR_3^o$−phenolate complex (*14*) gives evidence that phenol can, under some conditions, bind both to the phenolic pockets and to the His(B10) sites. By performing all our experiments in the presence of relatively high concentrations of PABA, we select for conditions where phenolate binding to the HisB10 R state sites is minimized. Furthermore, R state phenolate complexes are known to give distinctive UV−vis and CD spectral signatures in the Co(II) system. No hint of phenolate coordination was detected under the conditions of the experiments conducted herein. Although we have no such signatures for the HisB10 R state sites of the Zn(II) system, we do know a considerable amount about relative ligand affinities for these sites from the work of Huang et al. (*8*), and our conditions were selected to make phenolate binding at HisB10 negligible.

Table 1: Allosteric Parameters for the Zn(II)- and Co(II)-Substutited Wild-Type and E-A17Q Mutant Insulin Hexamers[a]

insulin species and phenolic and anionic ligands	$L_o^{A\,b,c}$	$L_o^{B\,b,c}$	$K_R^{o\,b,c}$ (x10^{-4} M)	$K_R^{b,c}$ (x10^{-4} M)	$r^{2\,b,c}$
WT Co(II) insulin and 2 mM PABA					
resorcinol	40 ± 20	$(3 \pm 1) \times 10^7$	2 ± 1	6 ± 3	0.99
phenol	40 ± 20	$(3 \pm 1) \times 10^7$	4 ± 2	2 ± 1	0.99
2,6-DHN	40 ± 20	$(3 \pm 1) \times 10^7$	1 ± 0.5	2 ± 1	0.98
WT Zn(II) insulin and 2 mM PABA					
resorcinol	5 ± 2	$(8 \pm 4) \times 10^5$	3 ± 1.5	8 ± 4	0.99
phenol	3 ± 1.5	$(8 \pm 4) \times 10^5$	7 ± 3.5	2 ± 1	0.97
2,6-DHN	5 ± 2	$(8 \pm 4) \times 10^5$	4 ± 2	2 ± 1	0.99
2,7-DHN	5 ± 2	$(8 \pm 4) \times 10^5$	4 ± 2	2 ± 1	0.99
A17Q Co(II) insulin and 2 mM PABA					
resorcinol	$(1 \pm 0.5) \times 10^2$	$(4 \pm 2) \times 10^7$	4 ± 2	1 ± 0.5	0.99
phenol	$(1 \pm 0.5) \times 10^2$	$(4 \pm 2) \times 10^7$	4 ± 2	2 ± 1	0.99
A17Q Zn(II) insulin and 2 mM PABA					
resorcinol	9 ± 4	$(1 \pm 0.5) \times 10^6$	4 ± 2	2 ± 1	0.99
phenol	9 ± 4	$(1 \pm 0.5) \times 10^6$	3 ± 1.5	8 ± 4	0.99

[a] The values for Zn(II)-substituted hexamers were determined from the 4H3N absorption changes as described in Figure 8. The values for the Co(II)-substituted hexamers were determined from the changes in the Co(II) d−d absorption bands (*2*−*4*). All experiments were performed at 25 °C in 50 mM Tris-ClO_4^- buffer at pH 8.0. [b] Parameters obtained from fits of the data to eq 1 (see the text). [c] The isotherms (see Figures 8 and 9) can be fit by more than one discrete set of values. Therefore, a set of high-correlation fits was determined by limiting each of the four variables such that only those values for the allosteric constants capable of fitting all of the data sets from different phenolic ligands for a given insulin species and a given anion concentration were allowed. Similarly, dissociation constants were limited to a range of values which could satisfactorily fit all of the data for a given phenolic compound. A nonlinear least-squares procedure (Peakfit) was used to determine values given for the four variables, L_o^A, L_o^B, K_R^o, and K_R (Figure 2). The goodness of fit is given by the reduced square of the residuals, r^2.

The qualitative results presented in Figure 9 indicate that the elimination of these salt bridges by mutation has negligible effects both on the magnitudes of the allosteric constants, L_o^A and L_o^B, and on the values of K_R and K_R^o. The absence of an effect of the mutation on the allosteric constants (Figure 2, eq 1, Table 1) indicates that the change in charge of A17 has little or no net effect on the conformational transition at pH 8.0. The pK_a values of peptide α-NH_3^+ groups that are not stabilized by salt bridging are generally in the range of ∼7.5 to 8.0, while salt bridging shifts the pK_a of the NH_3^+ group to higher values; e.g., the apparent pK_a for the salt bridge between the α-NH_3^+ of Ile16 and Asp194 in α-chymotrypsin is ∼8.8 (*27*, *28*), and the values for the intra- and intersubunit salt bridges in hemoglobin are elevated (*29*). Consequently, at pH 8.0, the A17−B1 salt bridge in wild-type T_6 should remain intact and the interaction with ArgB22 should be pH-independent below pH 10. If this is the case, then the apparent weakness of this salt bridge interaction may be explained by the fact that, at physiologically relevant ionic strengths, solvent-exposed ion pairs on protein surfaces usually are not much more stable than the separate ions. Indeed, ion pair formation in aqueous solution often does not contribute a net favorable standard free energy change to the stability of a folded polypeptide (*30*, *31*). Therefore, the free energy of stabilization of the T state by the A17−B1−B22 salt bridging at pH 8.0 may simply be small.[5]

Comparison of Co(II) and Zn(II) Wild-Type and GluA17Gln Insulin Hexamers in the Presence of 2 mM PABA. The distance between the phenolic pockets and the HisB10 sites together with the similarities of Zn(II) and Co(II) is likely to make negligible any site−site structural perturbations due to the substitution of Co(II) for Zn(II). Consequently, comparisons of the phenol, resorcinol, 2,6-DHN, and 2,7-DHN titrations for Co(II) and Zn(II) wild-type insulin hexamers by curve fitting to the fraction of R state (Figure 2, eq 1, Figure 8) were performed assuming that the affinities of the phenolic ligands obtained for the Co(II) insulin hexamer are unaffected by substitution of Zn(II) for Co(II).[4] When subjected to these constraints, isotherm fitting to eq 1 shows changes in L_o^A and in L_o^B of 10- and 35-fold, respectively, resulting from the substitution of Co(II) by Zn(II) (Table 1). These changes establish that the conversions from T_3T_3' to $T_3°R_3°$ and $T_3°R_3°$ to R_3R_3' are significantly more favorable for the Zn(II) insulin hexamer than for the Co(II)-substituted species. The more favorable value of L_o^A reduces the apparent sigmoidicity of the initial phase of the isotherm for the Zn(II) hexamer (compare the insets in panels A and B of Figure 8). Since the ratio of L_o^B/L_o^A ($\sim 1 \times 10^5$) remains essentially unchanged by the substitution of Co(II) for Zn(II), the tendency of the isotherms to plateau at $\rho = 0.5$ is not much affected.

The importance of the T to R state allosteric transition of the insulin hexamer to the physical and chemical stability of the hexamer in the production of formulations for use in the treatment of diabetics has been made apparent by recent studies. The relationship of the allosteric properties of the insulin hexamer to biological function is not known. We speculate that the enormous increase in the physical and chemical stability brought about by conversion to the R state in vitro reflects an in vivo function involving the stabilization of insulin within the secretory vesicles of the β-cell. If true, then it becomes of considerable interest to determine the identities of the biologically relevant allosteric ligands involved in stabilizing R state species. Work is now underway to isolate and identify these ligands.

In conclusion, our work shows that the chromophoric ligand, 4H3N, provides a sensitive probe both of ligand

[5] To predict the net effect of these salt bridges on the allosteric constants for the T to R state transition, the difference in the strengths of the interactions of B1, B22, and A17 with their respective microenvironments in the T and R states must be considered both for the mutant and for the wild-type species. Since the X-ray crystal structure of the mutant is not yet available, it is not possible to be sure if a less favorable interaction was introduced to the R state.

binding to the HisB10 metal ion sites (*8*) and of the T to R state allosteric transition of the zinc insulin hexamer. The titrations of Zn(II)- and Co(II)-substituted wild-type insulin hexamers by phenol, resorcinol, 2,6-DHN, and 2,7-DHN establish that the substitution of Co(II) for Zn(II) significantly alters the constants for the allosteric transition (Figure 8). Substitution of Co(II) for Zn(II) is predicted to affect the distribution of conformations through at least two different mechanisms. First, comparisons of the relative affinities of various ligands reveal that both monodentate anions (chloride ion and thiocyanate ion) and bidentate anions (various organic carboxylates) bind more weakly to the R state Co(II) hexamer than to the R state Zn(II) hexamer (*8*). Second, coordination to Co(II) occurs via an unfilled d shell, while coordination to Zn(II) occurs via an unfilled s shell.[3] Since there is no crystal field stabilization for Zn(II) complexes, coordination is nondirectional, while bonding to Co(II) is subject to crystal field effects. Therefore, the greater preference of the Co(II)-substituted hexamer compared to that of the Zn(II) species for an octahedral ligand field (and hence the T state) and the higher affinity of the Zn(II)−R state species for anionic ligands play important roles in determining the relative stabilities of the T and R states for the Co(II) and Zn(II) systems (*6*). While these effects combine to render the T to R state transition significantly more favorable for the Zn(II) system, the isotherms shown in Figures 4−9 establish that the Zn(II)-substituted hexamer is an allosteric protein that exhibits the same allosteric behavior, i.e., positive and negative cooperativity and apparent half-site reactivity, that has been documented for the Co(II)-substituted species (*2*−*4*).

ACKNOWLEDGMENT

We thank Ms. Susan E. Danielsen for assistance with the CD work, and we thank Sven E. Harnung for discussions concerning the interpretion of CD spectra.

REFERENCES

1. Kaarsholm, N. C., Ko, H.-C., and Dunn, M. F. (1989) *Biochemistry 28*, 4427−4435.
2. Bloom, C. R., Choi, W. E., Brzović, P. S., Ha, J. J., Huang, S.-T., Kaarsholm, N. C., and Dunn, M. F. (1995) *J. Mol. Biol. 245*, 324−330.
3. Bloom, C. R., Heymann, R., Kaarsholm, N. C., and Dunn, M. F. (1997) *Biochemistry 36*, 12746−12758.
4. Bloom, C. R., Kaarsholm, N. C., Ha, J., and Dunn, M. F. (1997) *Biochemistry 36*, 12759−12765.
5. Birnbaum, D. T., Dodd, S. W., Saxberg, B. E. H., Varshavsky, A. D., and Beals, J. M. (1996) *Biochemistry 35*, 5366−5378.
6. Rahuel-Clermont, S., French, C. A., Kaarsholm, N. C., and Dunn, M. F. (1997) *Biochemistry 36*, 5837−5845.
7. Brzović, P. S., Choi, W. E., Borchardt, D., Kaarsholm, N. C., and Dunn, M. F. (1994) *Biochemistry 33*, 13057−13069.
8. Huang, S. T., Choi, W. E., Bloom, C. R., Leuenberger, M., and Dunn, M. F. (1997) *Biochemistry 36*, 9878−9888.
9. Seydoux, F., Malhotra, O. P., and Bernhard, S. A. (1974) *CRC Crit. Rev. Biochem. 2*, 227−257.
10. Baker, E. N., Blundell, T. L., Cutfield, J. F., Cutfield, S. M., Dodson, E. J., Dodson, G. G., Hodgkin, D. C., Hubbard, R. E., Isaacs, N. W., Reynolds, C. D., Sakabe, K., Sakabe, N., and Vijayan, N. M. (1988) *Philos. Trans. R. Soc. London, Ser. B 319*, 369−456.
11. Derewenda, U., Derewenda, Z., Dodson, E. J., Dodson, G. G., Reynolds, C. D., Smith, G. D., Sparks, C., and Swensen, D. (1989) *Nature 338*, 594−596.
12. Ciszak, E., and Smith, G. D. (1994) *Biochemistry 33*, 1512−1517.
13. Smith, G. D., and Dodson, G. G. (1992) *Biopolymers 32*, 1749−1756.
14. Smith, G. D., and Dodson, G. G. (1992) *Proteins: Struct., Funct., Genet. 14*, 401−408.
15. Bentley, G. A., Brange, J., Derewenda, Z., Dodson, E. J., Dodson, G. G., Markussen, J., Wilkinson, A. J., Wollmer, A., and Xaio, B. (1992) *J. Mol. Biol. 228*, 1163−1176.
16. Whittingham, J. L., Chaudhuri, S., Dodson, E. J., Moody, P. C. E., and Dodson, G. G. (1995) *Biochemistry 34*, 15553−15563.
17. Roy, M., Brader, M. L., Lee, R. W.-K., Kaarsholm, N. C., Hansen, J., and Dunn, M. F. (1989) *J. Biol. Chem. 264*, 19081−19085.
18. Choi, W. E., Brader, M. L., Aguilar, V., Kaarsholm, N. C., and Dunn, M. F. (1993) *Biochemistry 32*, 11638−11645.
19. Choi, W. E., Borchardt, D., Kaarsholm, N. C., Brzovic, P. S., and Dunn, M. F. (1996) *Proteins: Struct., Funct., Genet. 26*, 377−390.
20. Blundell, T., Dodson, G., Hodgkin, D., and Mercola, D. (1972) *Adv. Protein Chem. 26*, 279−402.
21. Smith, G. D., Swenson, D. C., Dodson, E. J., Dodson, G. G., and Reynolds, C. D. (1984) *Proc. Natl. Acad. Sci. U.S.A. 81*, 7093−7079.
22. Brader, M. L., Kaarsholm, N. C., Lee, W.-K., and Dunn, M. F. (1991) *Biochemistry 30*, 6636−6645.
23. Brader, M. L., Borchardt, D., and Dunn, M. F. (1992) *J. Am. Chem. Soc. 114*, 4480−4486.
24. Brader, M. L., Borchardt, D., and Dunn, M. F. (1992) *Biochemistry 31*, 4691−4696.
25. Brader, M. L., Kaarsholm, N. C., Harnung, S. E., and Dunn, M. F. (1997) *J. Biol. Chem. 272*, 1088−1094.
26. Porter, R. R. (1953) *Biochem. J. 53*, 320−328.
27. Oppenheimer, H. L., Labouesse, B., and Hess, G. P. (1966) *J. Biol. Chem. 241*, 2720−2730.
28. Fersht, A. R., and Requena, Y. (1971) *J. Mol. Biol. 60*, 279−290.
29. Perutz, M. F. (1989) *Q. Rev. Biophys. 22*, 139−236.
30. Kyte, J. (1995) *Structure in Protein Chemistry*, p 157, Garland Publishing Co., New York.
31. Blasie, C. A., and Berg, J. M. (1997) *Biochemistry 36*, 6218−6222.

BI980071Z